Pyrazino[2,3-*g*]quinoxaline-2,7-dione based π-conjugated polymers with affinity towards acids and semiconductor performance in organic thin film transistors

Jesse Quinn, Chang Guo, Lewis Ko, Bin Sun, Yinghui He and Yuning Li*
Department of Chemical Engineering and Waterloo Institute of Nanotechnology (WIN), University of Waterloo, 200 University Avenue West, Waterloo, Ontario, Canada N2L 3G1

Email: yuning.li@uwaterloo.ca

Additional data

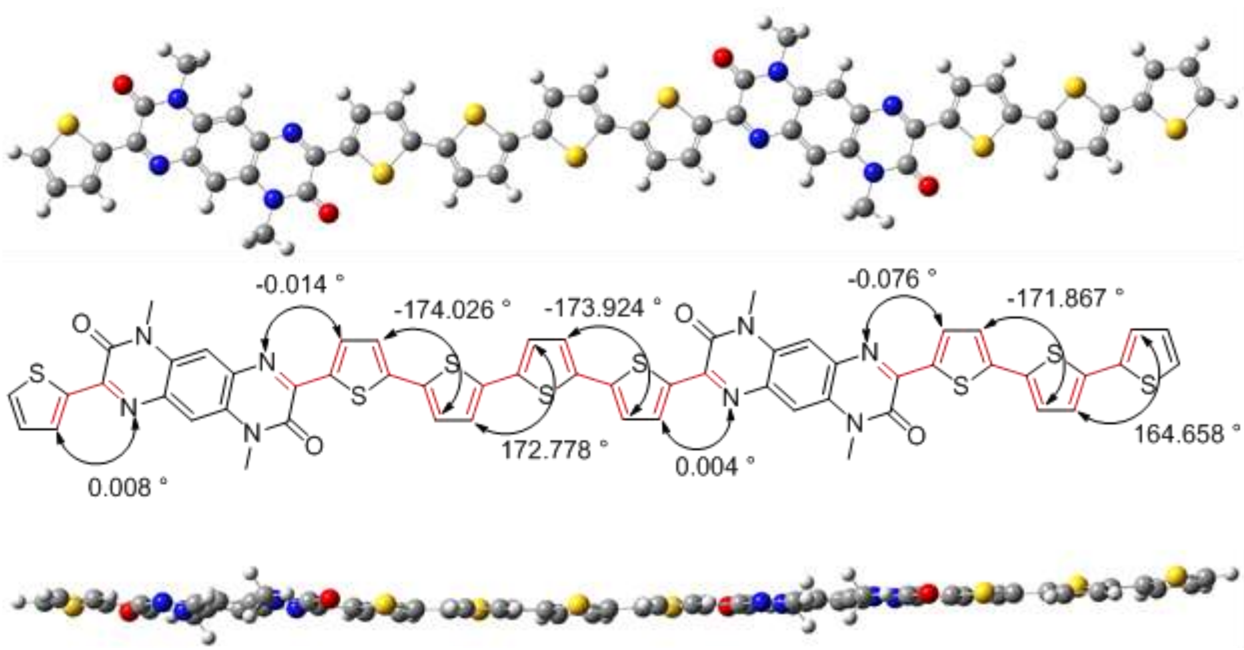

Fig. S1 The optimized geometry and dihedral angles of the **PQx2T-BT-Me** dimer using Gaussian 09 Revision D.01[1] with the B3LYP/6-31G(d) level of theory under tight convergence.

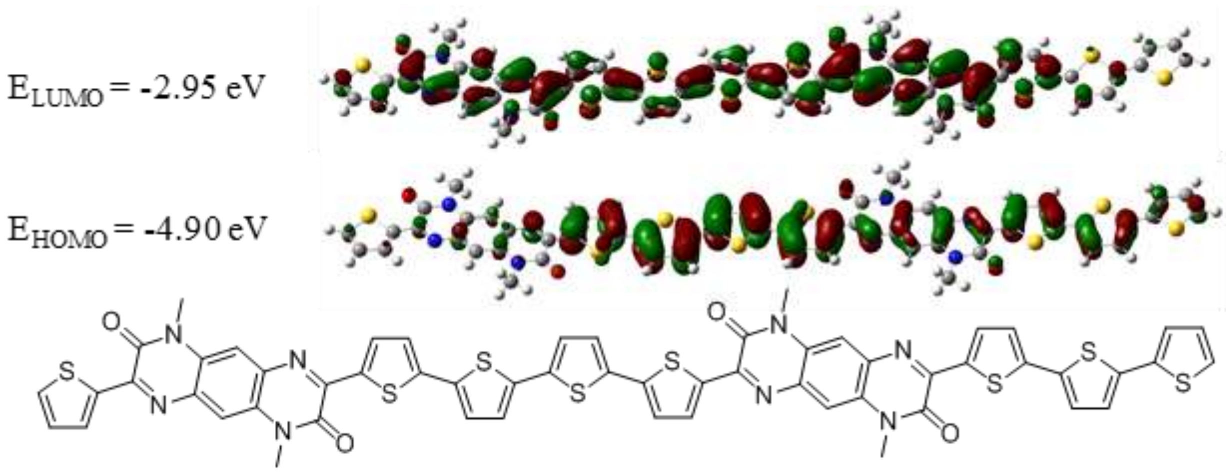

PQx2T-BT-Me dimer

Fig. S2 The optimized LUMO and HOMO wavefunction distributions of the **PQx2T-BT-Me** dimer using Gaussian 09 Revision D.01[1] with the B3LYP/6-31G(d) level of theory under tight convergence.

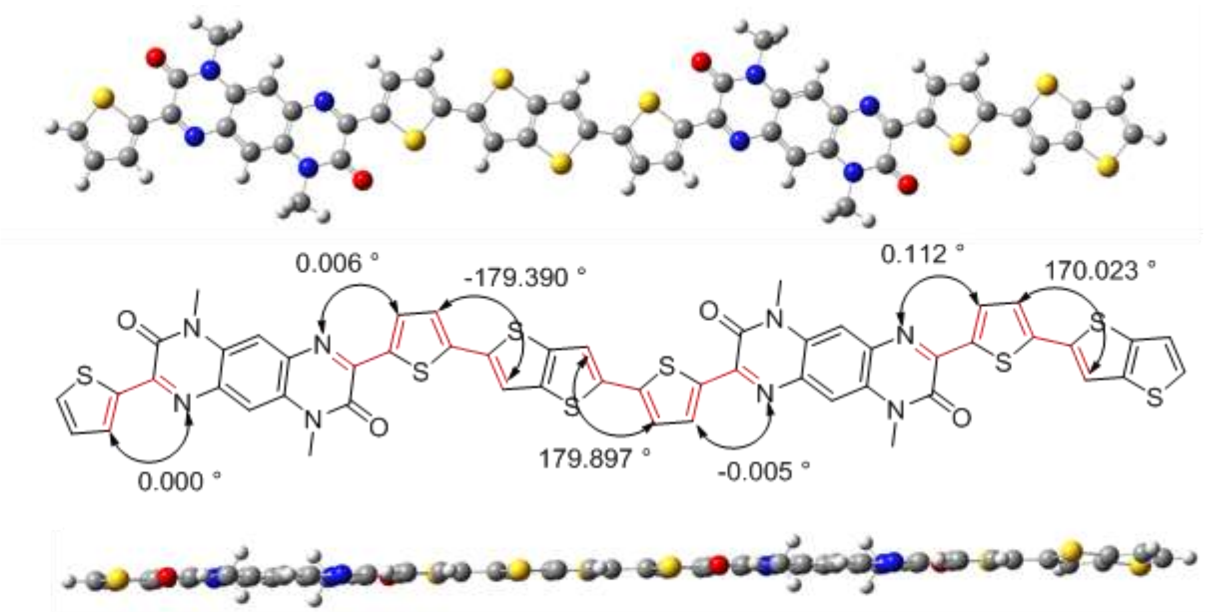

Fig. S3 The optimized geometry and dihedral angles of the **PQx2T-TT-Me** dimer using Gaussian 09 Revision D.01[1] with the B3LYP/6-31G(d) level of theory under tight convergence.

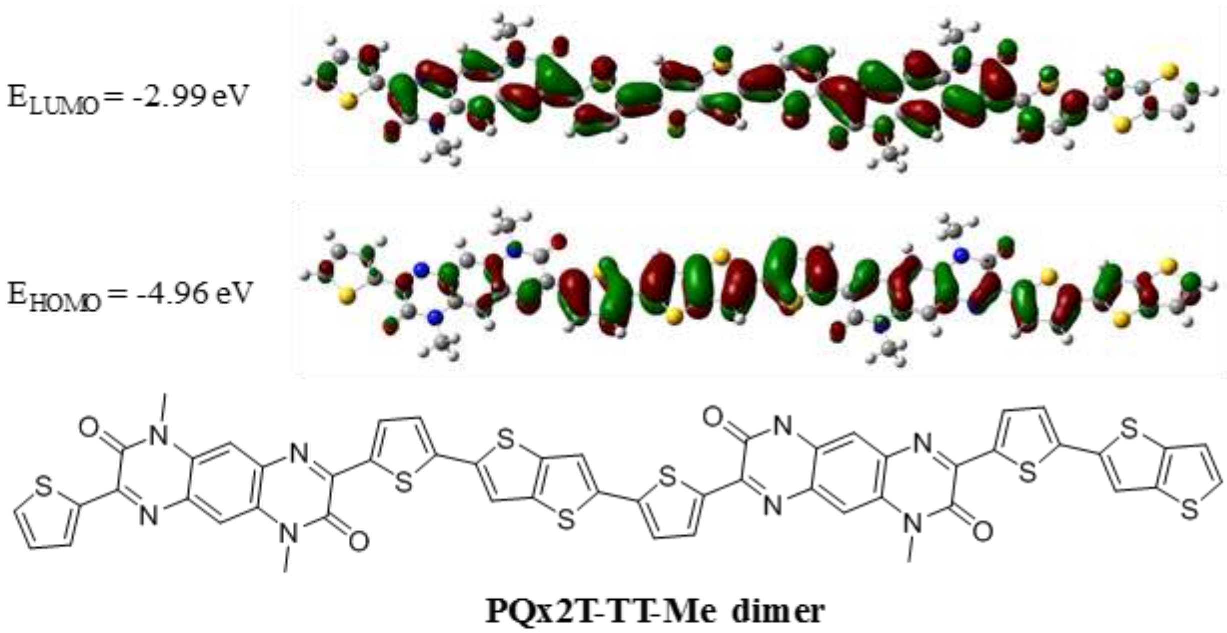

Fig. S4 The optimized LUMO and HOMO wavefunction distributions of the **PQx2T-TT-Me** dimer using Gaussian 09 Revision D.01[1] with the B3LYP/6-31G(d) level of theory under tight convergence.

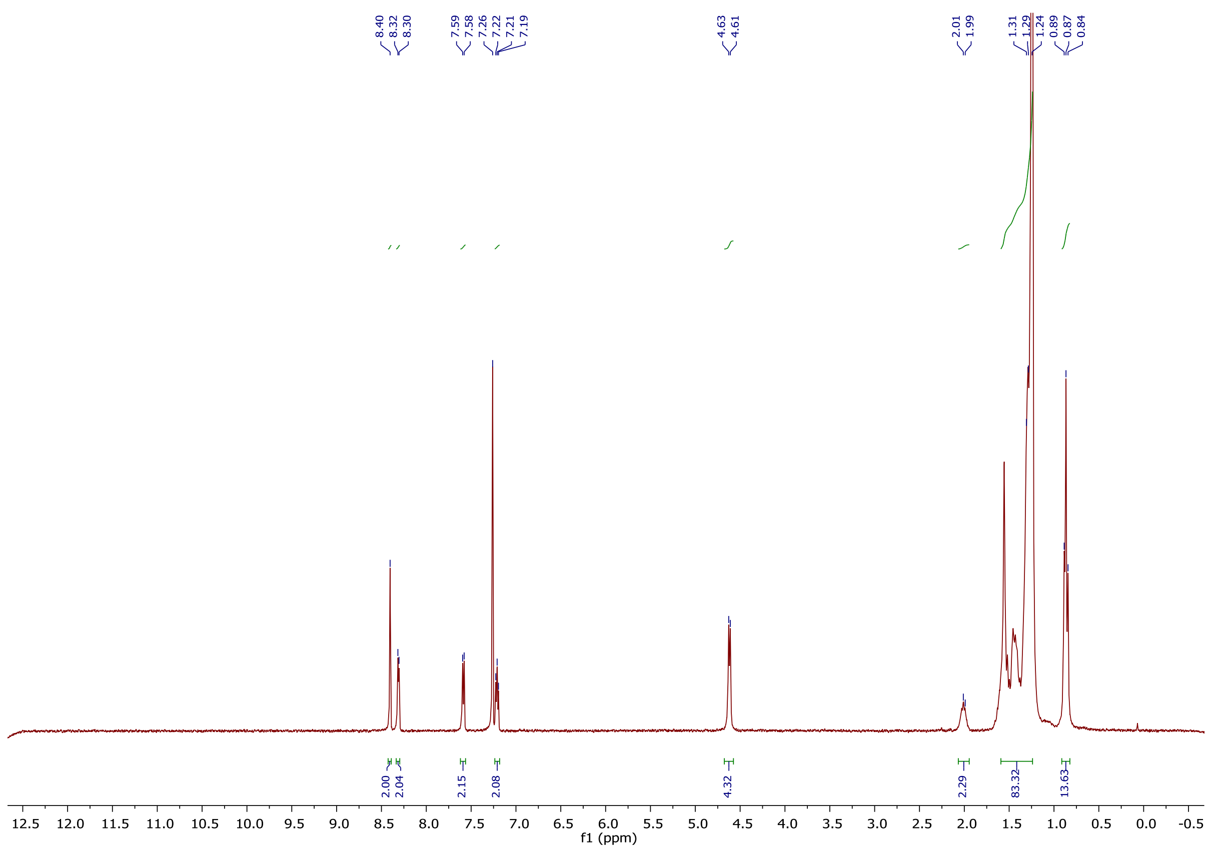

Fig. S5 300 MHz ^{1}H NMR spectrum for 1,6-bis(2-decyltetradecyl)-3,8-di(thiophen-2-yl)-1,6-dihydropyrazino[2,3-*g*]quinoxaline-2,7-dione (**PQx2T-24**) in $CDCl_3$.

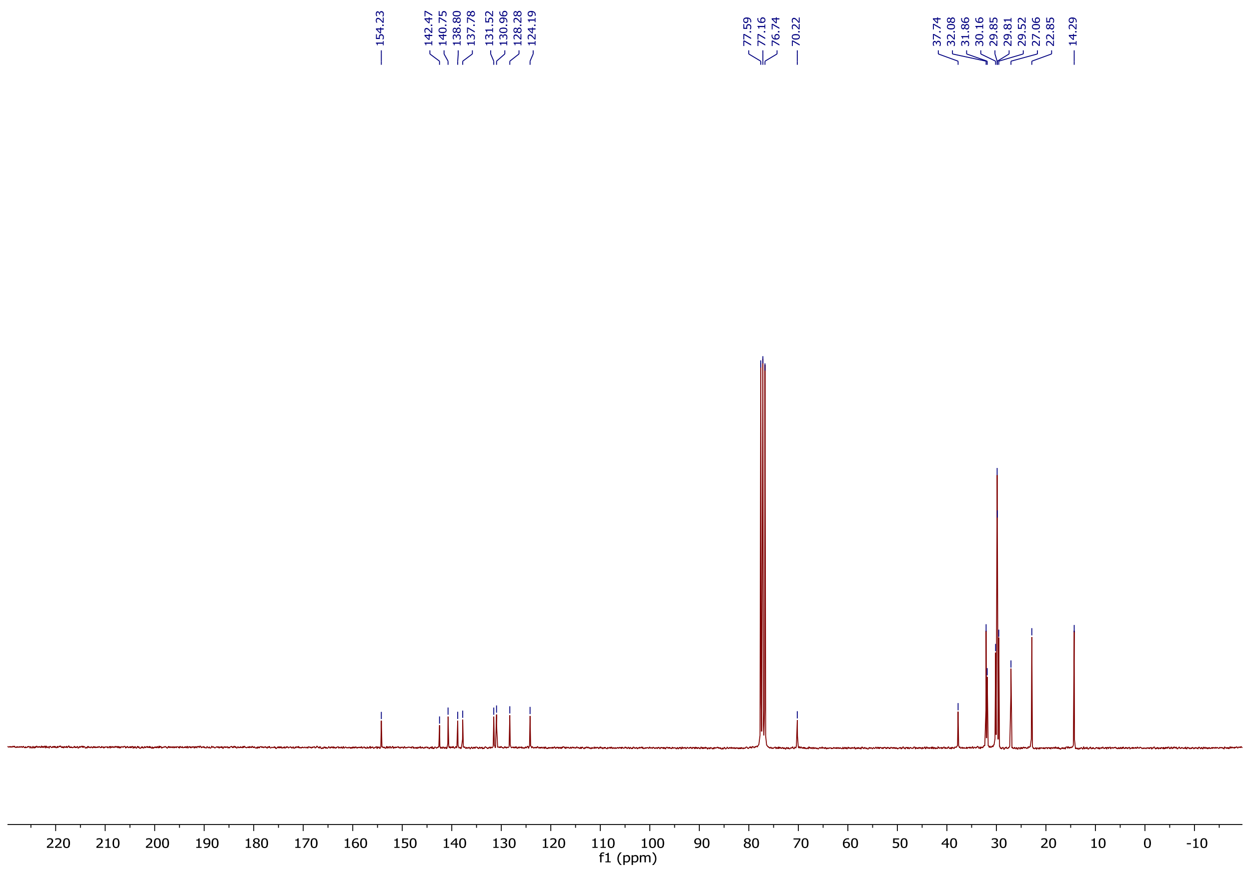

Fig. S6 75 MHz ^{13}C NMR spectrum for 1,6-bis(2-decyltetradecyl)-3,8-di(thiophen-2-yl)-1,6-dihydropyrazino[2,3-*g*]quinoxaline-2,7-dione (**PQx2T-24**) in $CDCl_3$.

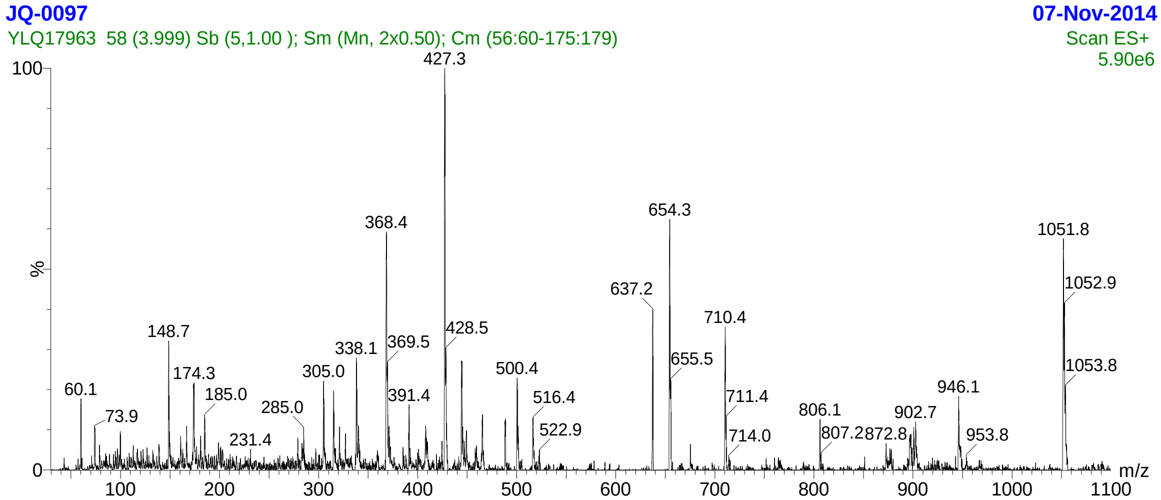

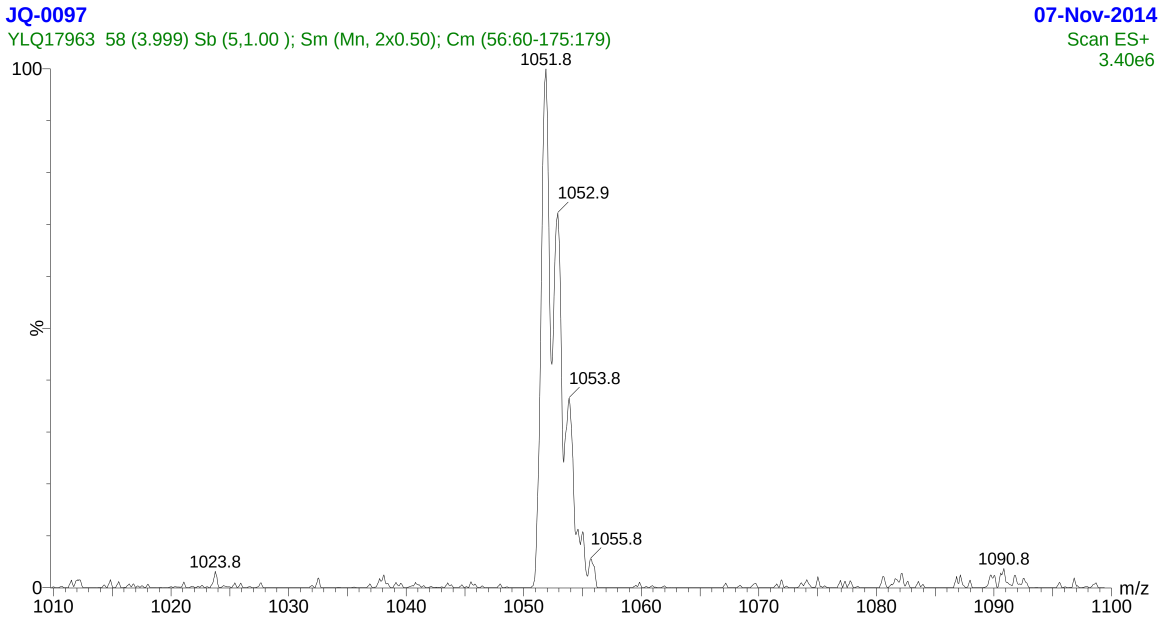

Fig. S7 The MS (ESI+) [M+H]+ spectra for 1,6-bis(2-decyltetradecyl)-3,8-di(thiophen-2-yl)-1,6-dihydropyrazino[2,3-*g*]quinoxaline-2,7-dione (**PQx2T-24**).

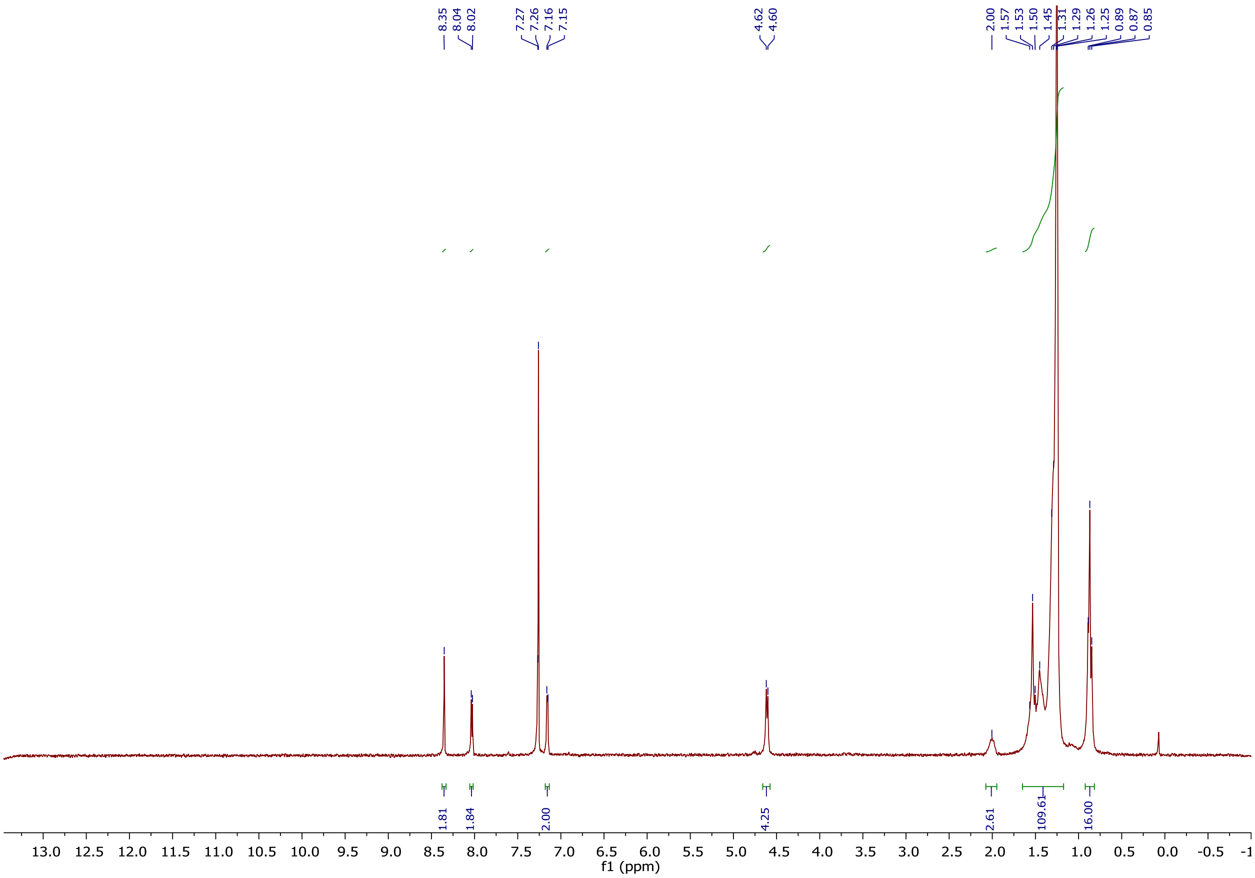

Fig. S8 300 MHz ^{1}H NMR spectrum for 3,8-bis(5-bromothiophen-2-yl)-1,6-bis(2-decyltetradecyl)-1,6-dihydropyrazino[2,3-*g*]quinoxaline-2,7-dione (**PQx2T-Br-24**) in $CDCl_3$.

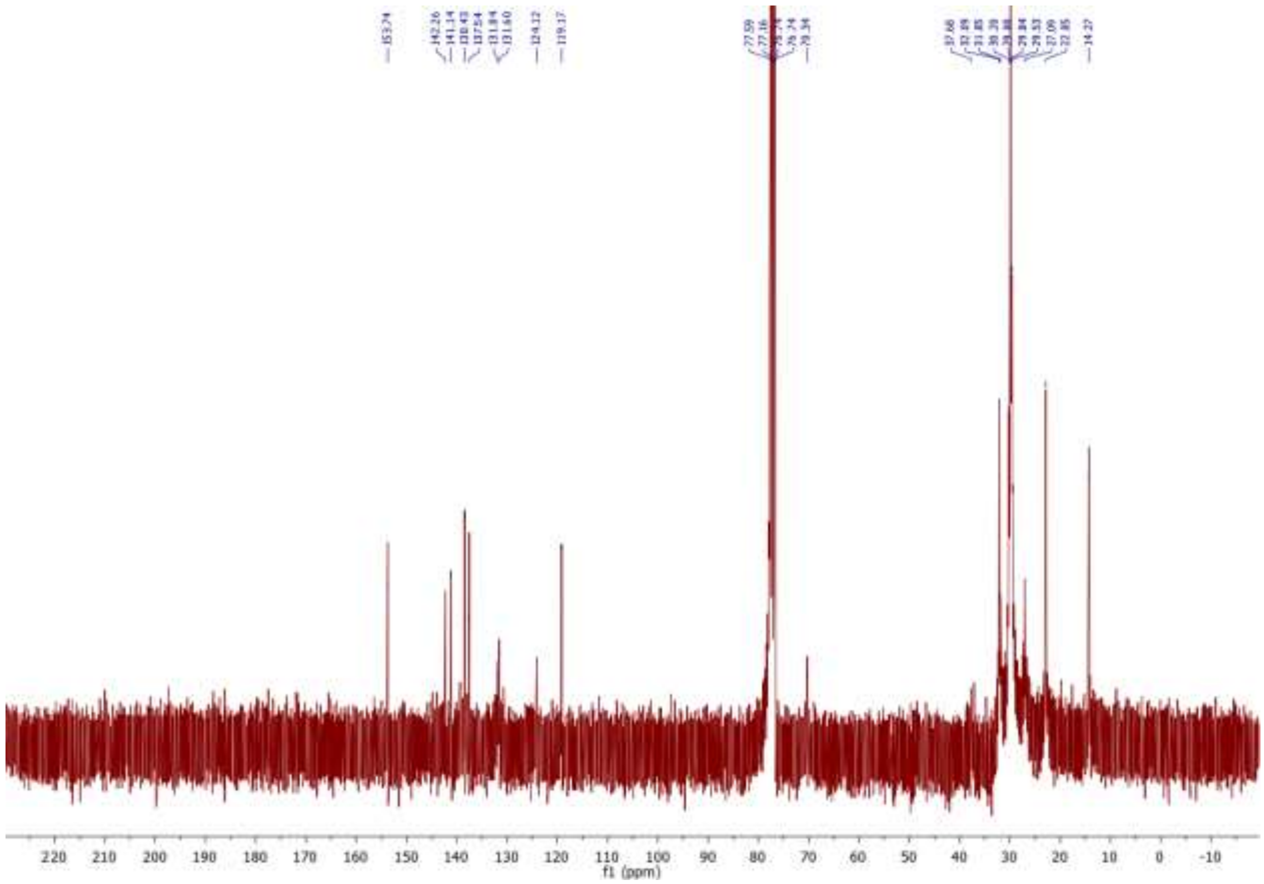

Fig. S9 75 MHz ^{13}C NMR spectrum for 3,8-bis(5-bromothiophen-2-yl)-1,6-bis(2-decyltetradecyl)-1,6-dihydropyrazino[2,3-*g*]quinoxaline-2,7-dione (**PQx2T-Br-24**) in $CDCl_3$.

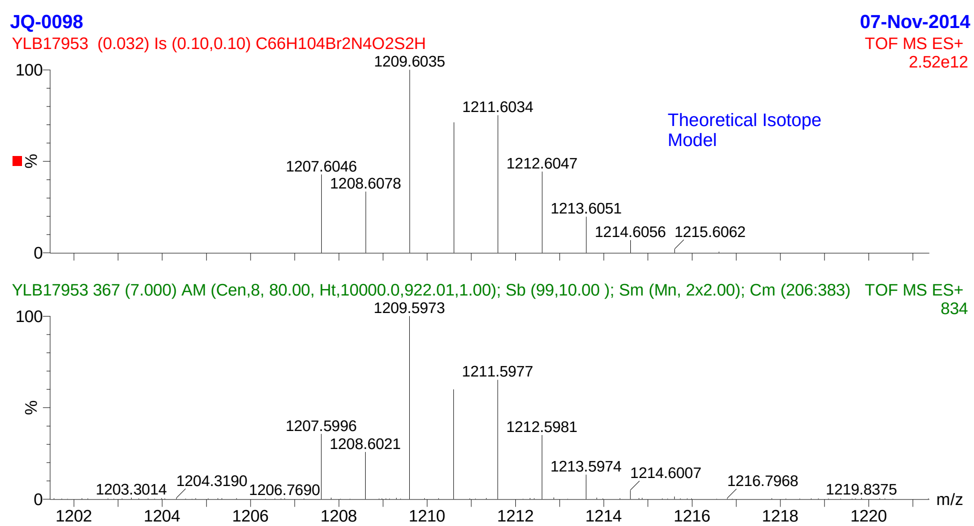

Fig. S10 The HR-MS (ESI+) (M+H)+ spectra for 3,8-bis(5-bromothiophen-2-yl)-1,6-bis(2-decyltetradecyl)-1,6-dihydropyrazino[2,3-*g*]quinoxaline-2,7-dione (**PQx2T-Br-24**).

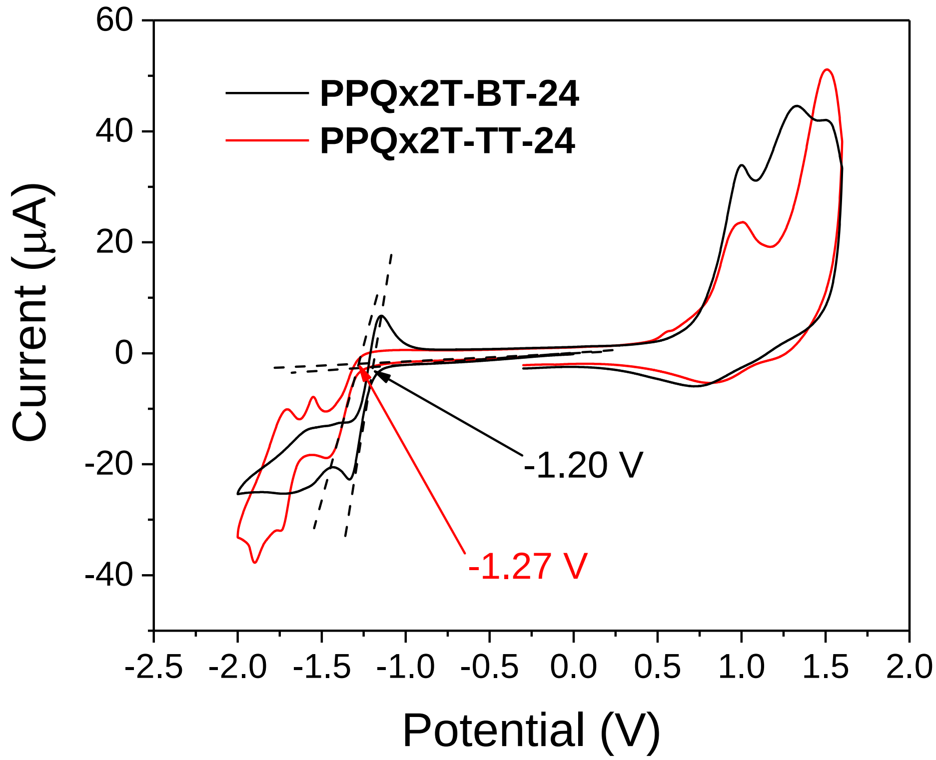

Fig. S11 Cyclic voltammograms of polymers in a 0.1 M tetrabutylammonium hexafluorophosphate solution under nitrogen in dry acetonitrile at a scan rate of 50 mV s^{-1}.

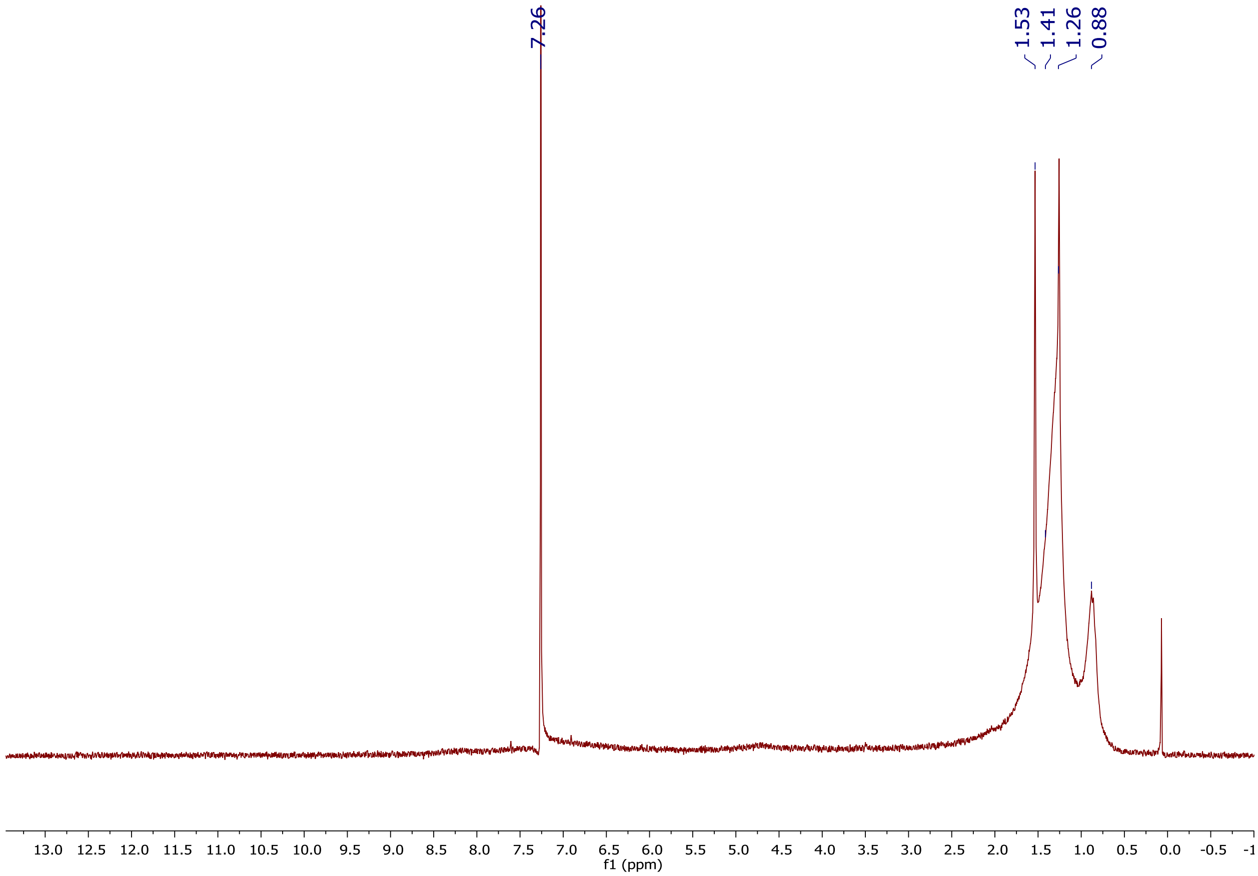

Fig. S12 300 MHz ^{1}H NMR spectrum for **PPQx2T-BT-24** in $CDCl_3$.

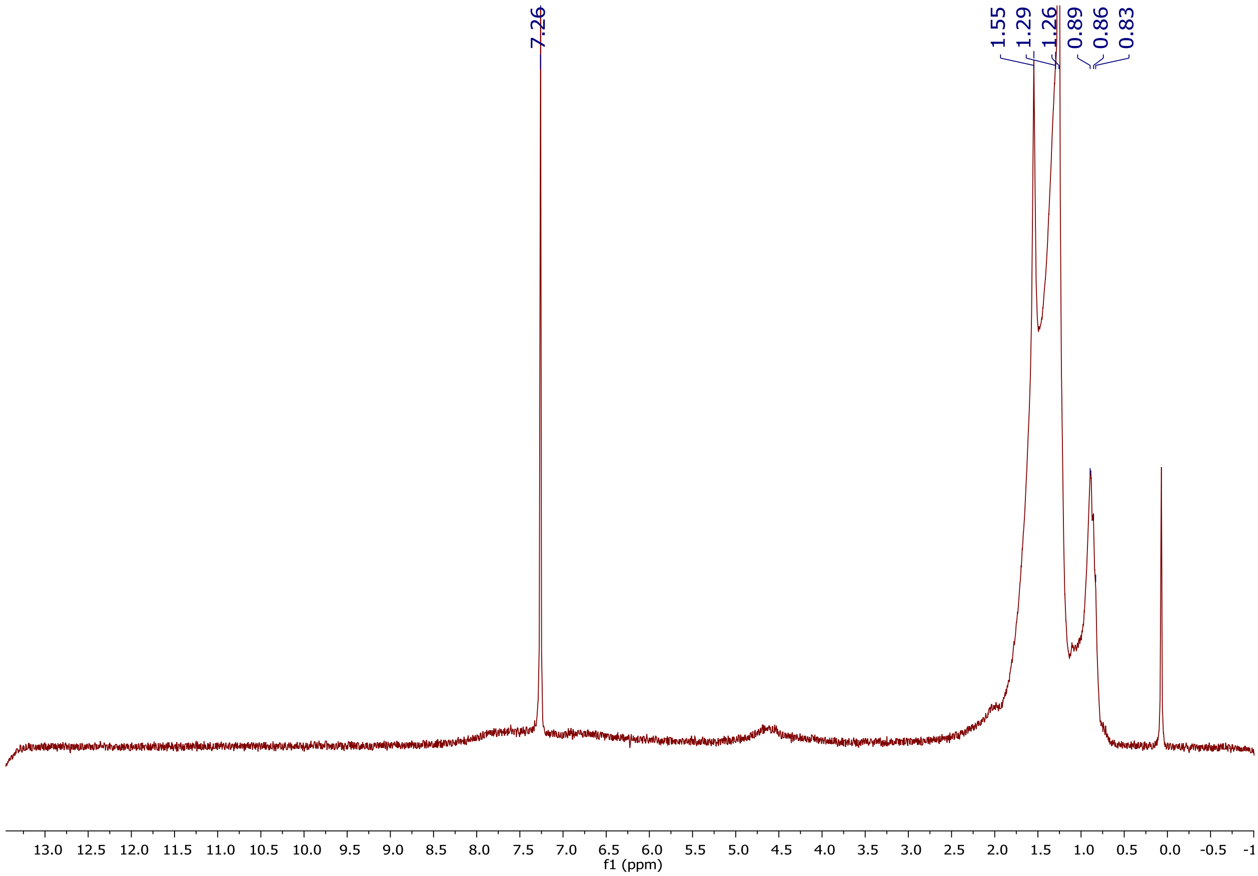

Fig. S13 300 MHz ^{1}H NMR spectrum for **PPQx2T-TT-24** in $CDCl_3$.

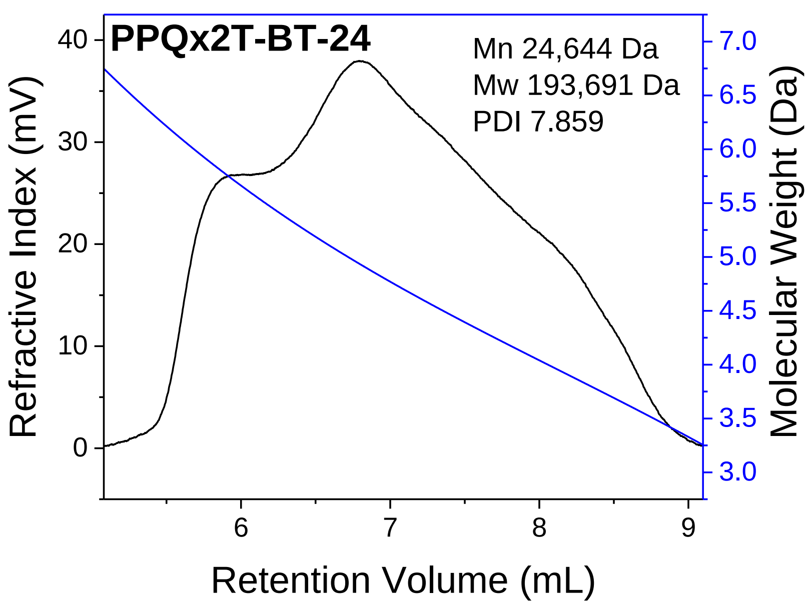

Fig. S14 High temperature GPC traces of **PPQx2T-BT-24** with refractive index detector.

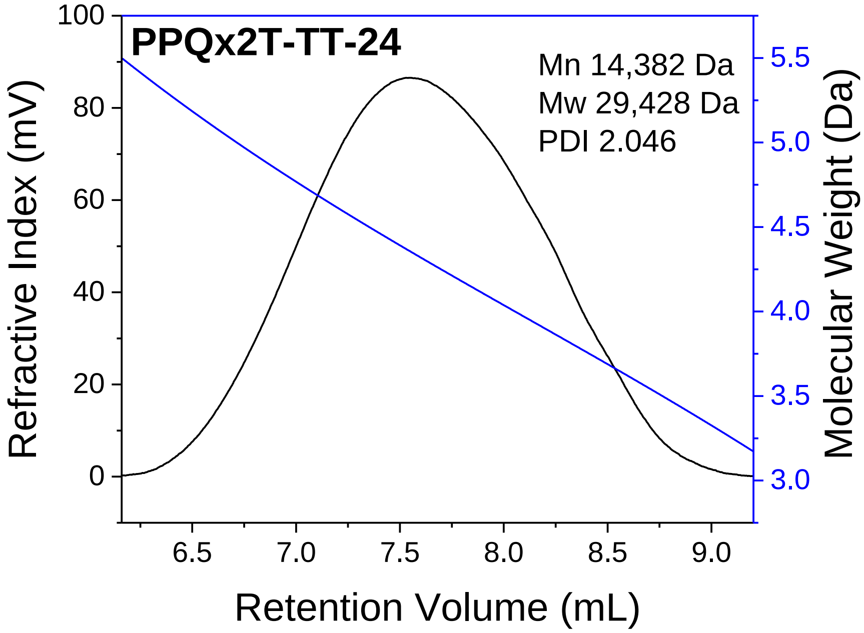

Fig. S15 High temperature GPC traces of **PPQx2T-TT-24** with refractive index detector.

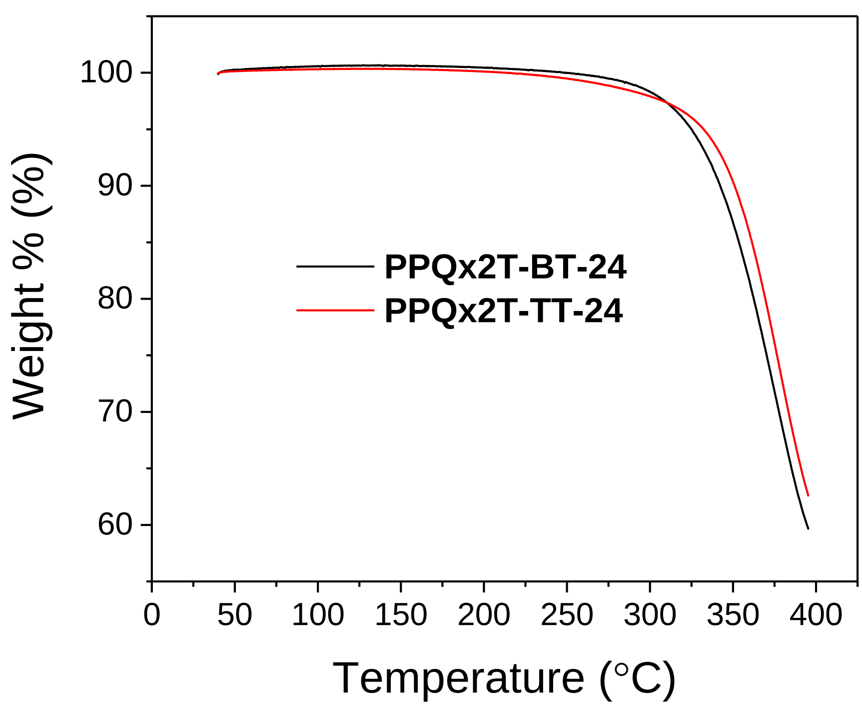

Fig. S16 TGA curves of **PPQx2T-BT-24** and **PPQx2T-TT-24** with a heating rate of 10 °C min^{-1} under nitrogen.

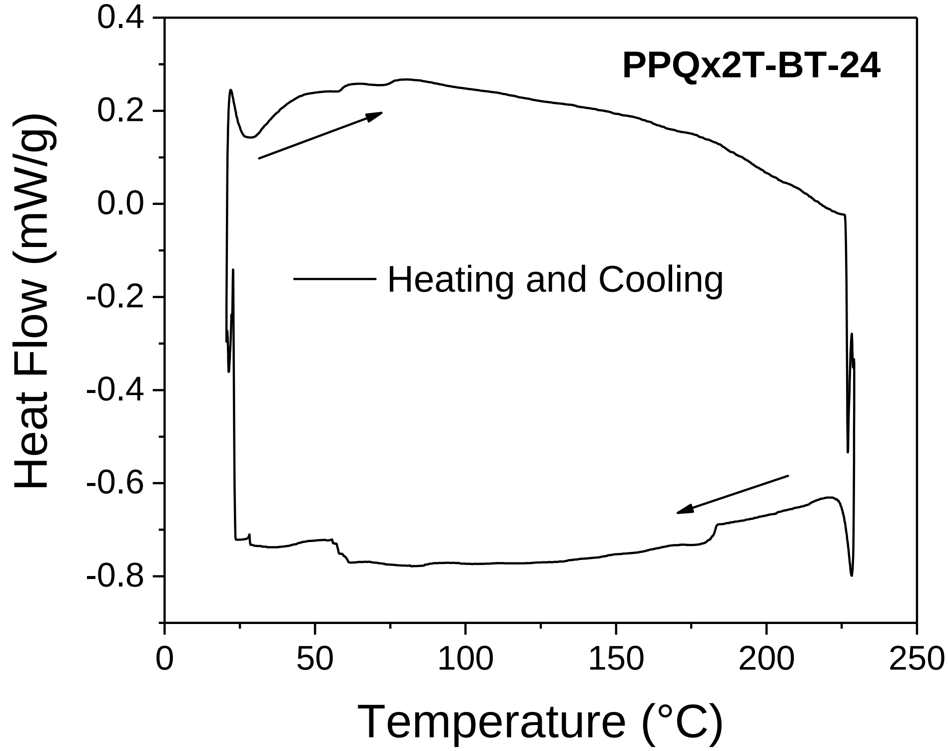

Fig. S17 DSC thermogram of **PPQx2T-BT-24** at a heating rate of 20 °C min^{-1} under nitrogen.

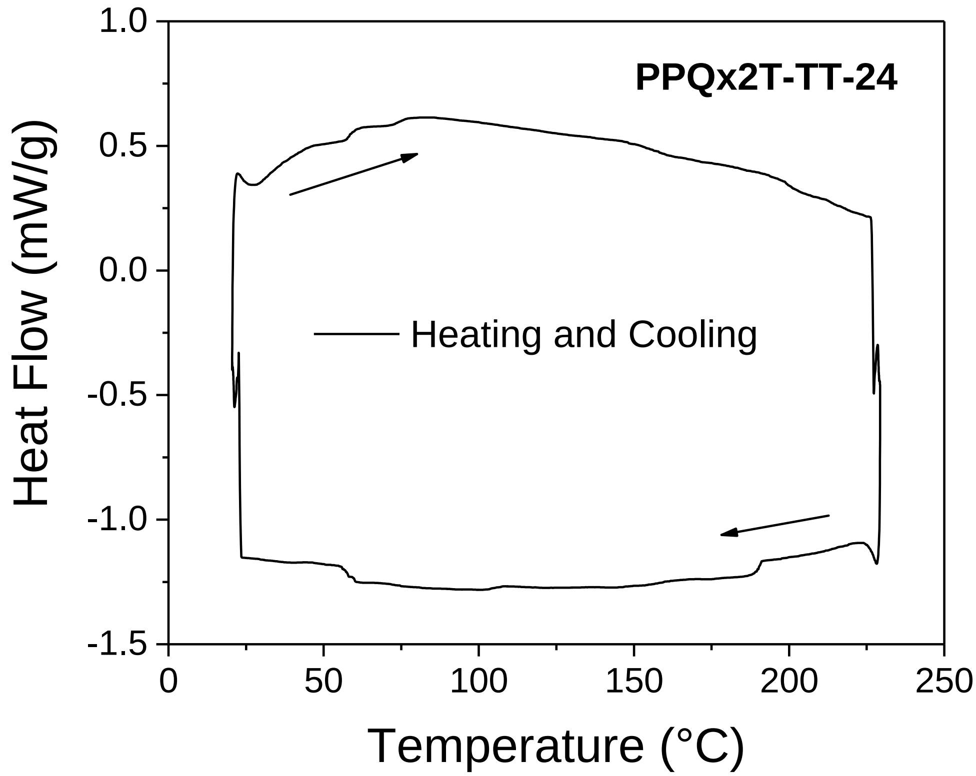

Fig. S18 DSC thermogram of **PPQx2T-TT-24** at a heating rate of 20 °C min^{-1} under nitrogen.

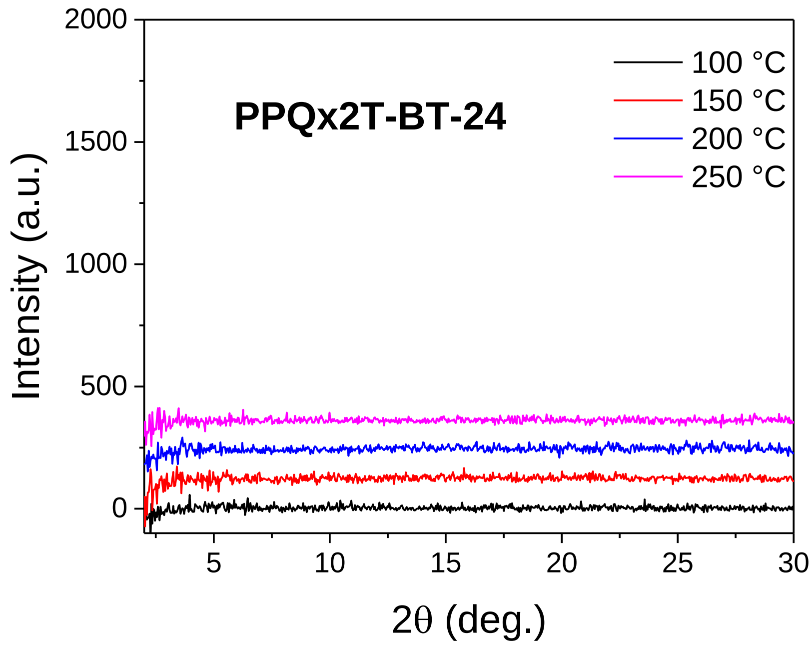

Fig. S19 XRD diagram obtained in the reflection mode for the spin-coated **PPQx2T-BT-24** thin film on silicon substrates annealed at 100, 150, 200, and 250 °C.

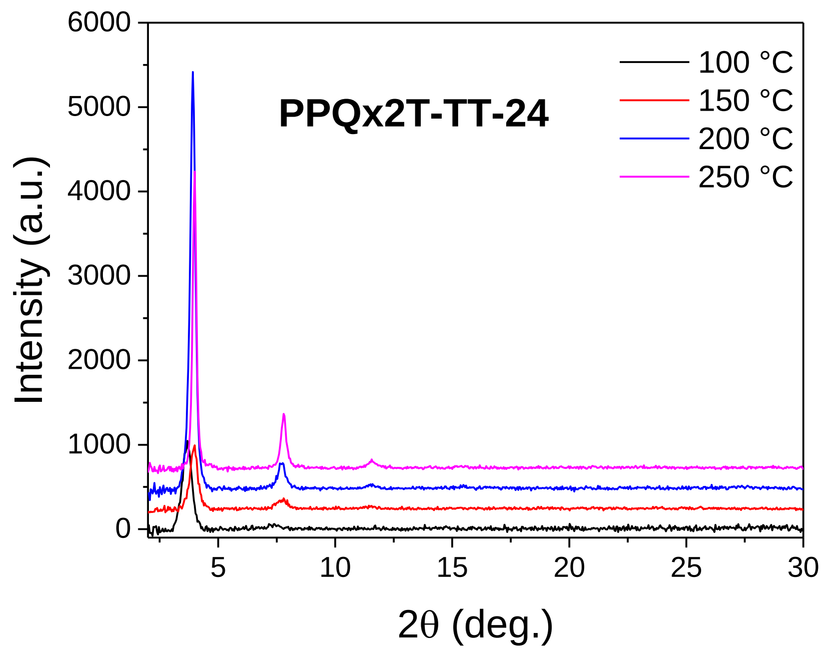

Fig. S20 XRD diagram obtained in the reflection mode for the spin-coated **PPQx2T-TT-24** thin film on silicon substrates annealed at 100, 150, 200, and 250 °C.

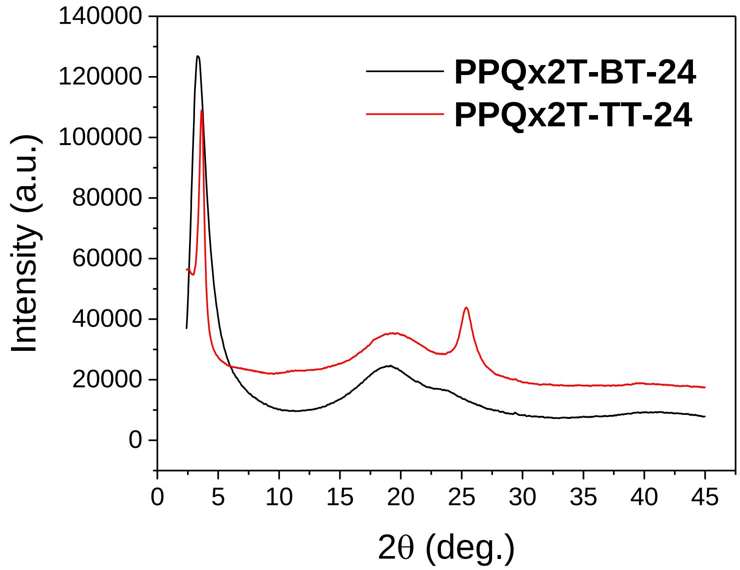

Fig. S21 XRD diagrams obtained in the transmission mode for **PPQx2T-BT-24** and **PPQx2T-TT-24** polymer flakes.

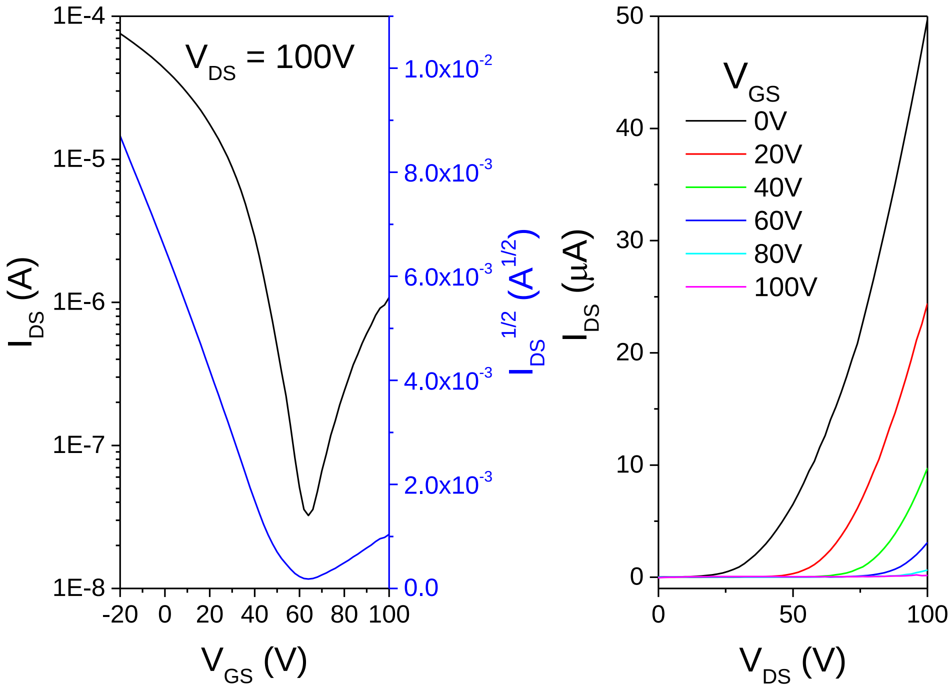

Fig. S22 The transfer (left) and output curves (right) of a typical OTFT device with a **PPQx2T-TT-24** thin film annealed at 200 °C. Device dimensions: channel width (*W*) = 1000 μm; channel length (*L*) = 30 μm.

Table S1 The summary of OTFT performance of **PPQx2T-BT-24** and **PPQx2T-TT-24**.

Polymer	Annealing temperature (°C)	Hole mobility[a] (10^{-3} $cm^2V^{-1}s^{-1}$)	Electron mobility[a] (10^{-3} $cm^2V^{-1}s^{-1}$)	Average V_{th} (V) p-/n-channel	I_{on}/I_{off}[b]
PPQx2T-BT-24	100	0.42 (0.38 ± 0.03)	4.62 (3.99 ± 0.46)	-23.06/44.12	~10^2
	150	0.47 (0.48 ± 0.02)	4.47 (3.94 ± 0.40)	-25.63/49.68	~10^2
	200	0.52 (0.50 ± 0.02)	4.28 (3.97 ± 0.31)	-30.47/42.42	~10^2
	250	0.31 (0.28 ± 0.03)	2.84 (2.62 ± 0.25)	-50.49/43.48	~10^2
PPQx2T-TT-24	100	16.20 (12.90 ± 1.89)	0.14 (0.12 ± 0.05)	-23.83/79.48	~10^5
	150	42.00 (34.10 ± 5.46)	2.95 (2.81 ± 0.20)	-19.45/66.36	~10^5
	200	48.20 (37.90 ± 6.75)	3.95 (3.12 ± 0.98)	-20.29/62.63	~10^5
	250	36.60 (27.30 ± 6.53)	2.09 (1.30 ± 0.58)	-22.14/63.11	~10^5

[a] The maximum (average ± standard deviation) mobility was calculated from the saturated regime of at least five devices for each condition. [b] Only p-channel data are reported for **PPQx2T-TT-24**.

Table S2 The summary of UV-Vis absorption of various acids for **PPQx2T-BT-24** and **PPQx2T-TT-24**.

Polymer	TFA		BBr_3	
	Conc.	λ_{max}, nm	Conc.	λ_{max}, nm
PPQx2T-BT-24	0	600	0	600
	1 mM	600	1 μM	605
	10 mM	602		
	50 mM	604		
	100 mM	607		
	500 mM	818(sh)		
	1 M	834		
	2 M	846	4 μM	621(sh)
PPQx2T-TT-24	0	627	0	627
	1 mM	626	1 μM	768(sh)
	5 mM	617		
	10 mM	615		
	50 mM	786		
	100 mM	804		
	500 mM	896		
	1 M	908		
	2 M	914	6 μM	846

References

1 M. J. Frisch, G. W. Trucks, H. B. Schlegel, G. E. Scuseria, M. A. Robb, J. R. Cheeseman, G. Scalmani, V. Barone, B. Mennucci, G. A. Petersson, H. Nakatsuji, M. Caricato, X. Li, H. P. Hratchian, A. F. Izmaylov, J. Bloino, G. Zheng, J. L. Sonnenberg, M. Hada, M. Ehara, K. Toyota, R. Fukuda, J. Hasegawa, M. Ishida, T. Nakajima, Y. Honda, O. Kitao, H. Nakai, T. Vreven, J. A. Montgomery Jr., J. E. Peralta, F. Ogliaro, M. J. Bearpark, J. Heyd, E. N. Brothers, K. N. Kudin, V. N. Staroverov, R. Kobayashi, J. Normand, K. Raghavachari, A. P. Rendell, J. C. Burant, S. S. Iyengar, J. Tomasi, M. Cossi, N. Rega, N. J. Millam, M. Klene, J. E. Knox, J. B. Cross, V. Bakken, C. Adamo, J. Jaramillo, R. Gomperts, R. E. Stratmann, O. Yazyev, A. J. Austin, R. Cammi, C. Pomelli, J. W. Ochterski, R. L. Martin, K. Morokuma, V. G. Zakrzewski, G. A. Voth, P. Salvador, J. J. Dannenberg, S. Dapprich, A. D. Daniels, Ö. Farkas, J. B. Foresman, J. V. Ortiz, J. Cioslowski and D. J. Fox, *Gaussian 09 Revision D.01*, Gaussian, Inc., Wallingford, CT, USA, 2009.